South African Journal for Science and Technology
ISSN: (Online) 2222-4173, (Print) 0254-3486

Differential response of photosynthetic electron transport and CO_2 assimilation in sensitive (S156) and resistant (R123) *Phaseolus vulgaris* L. (bush bean) genotypes to chronic ozone exposure

Author:
Gert HJ Krüger[1*],
Cornelius CW Scheepers[1],
Reto J Strasser[1,2],
Jacques M Berner

Affiliations:
[1] Unit for Environmental Sciences and Management, North-West University, Potchefstroom, South Africa

[2] Laboratory of Bioenergetics, University of Geneva, Switserland

Corresponding author:
Gert H.J. Krüger
E-mail:
gert.kruger@nwu.ac.za

Dates:
Received: 02/09/2017
Accepted: 05/11/2018
Published:

How to cite this article:
Gert HJ Krüger, Cornelius CW Scheepers, Reto J Strasser, Jacques M Berner, Differential response of photosynthetic electron transport and CO_2 assimilation in sensitive (*S156*) and resistant (*R123*) *Phaseolus vulgaris* L. (bush bean) genotypes to chronic ozone exposure, *Suid-Afrikaanse Tydskrif vir Natuurwetenskap en Tegnologie* 37(1) (2018)

'n Afrikaanse vertaling van die manuskrip is aanlyn beskikbaar by http://www.satnt.ac.za/index.php/satnt/article/view/684

Tropospheric ozone is currently regarded as one of the most important air pollutants, since it causes more damage to vegetation world-wide than all the other pollutants combined (Ashmore and Bell 1991). Due to its oxidative nature ozone causes leaf damage and a decrease in photosynthesis. Ozone tolerance varies widely between species and genotypes. The aim of this study was to identify and quantify the physiological and biochemical constraints imposed by chronic ozone exposure of two bush bean (*Phaseolus vulgaris* L.) genotypes with known difference in sensitivity, namely *S156* (sensitive) and *R123* (resistant), to charcoal-filtered air and 80 nmol.mol^{-1} O_3. The study was conducted in open-top growth chambers (OTCs) over the entire growth period by measuring chlorophyll *a* fluorescence (JIP-test) and photosynthetic gas exchange of the test plants weekly. The status of the photosynthetic apparatus was assessed by analysis of chlorophyll *a* fluorescence kinetics (JIP test) and CO_2 response curves (*A*:C_i). O_3-induced physiological effects were detected in *S156* long before appearance of necrotic spots on the trifoliate leaves. Photosynthesis was substantially inhibited in *S156*, mainly due to disengagement of the oxygen evolving complex (OEC), inhibition of intersystem electron transport and the reduction of end-electron acceptors of PSI (ferredoxin, NADP$^+$), causing the concomitant decrease in the carboxylation and regeneration of ribulose-1,5-bisphosphate. Seed and pod yield closely reflected the photosynthetic response of the test plants.

Although leaves of both the genotypes were affected visually, it was *S156* that displayed severe necrotic ozone injury on the trifoliate leaves. Our data contribute to and complement the existing knowledge on the processes underlying the phytotoxicity of O_3 needed for development of tolerant genotypes.

Keywords: *Phaseolus vulgaris*, ozone, photosynthesis, chlorophyll *a* fluorescence, gas exchange, photosynthetic electron transport, seed yield, open-top chambers.

Kontrasterende invloed van chroniese osoonblootstelling op fotosintetiese elektronoordrag en CO_2-assimilering in gevoelige (S156) en bestande (R123) Phaseolus vulgaris L. genotipes: Troposferiese osoon (O_3) word beskou as een van die belangrikste lugbesoedelstowwe aangesien dit wêreldwyd meer skade aan landbougewasse aanrig as al die ander besoedelstowwe saam. Weens die oksiderende aard daarvan veroorsaak O_3 blaarskade en ´n afname in fotosintese. Bestandheid van gewasse teen O_3 verskil aansienlik tussen spesies en genotipes. Met hierdie studie is nuwe inligting oor die fisiologiese en biochemiese grondslag van die skadelike effek van O_3 verkry deur chroniese blootstelling van twee bosboongenotipes met bekende gevoeligheid vir O_3, naamlik *S156* (gevoelig) en *R123* (bestand), aan onderskeidelik houtskool-gefiltreerde lug en 80 dpm O_3. Die studie is uitgevoer in oop-dek-groeikamers (OTCs) vir die volle groeiperiode tot wasdom. Die status van die fotosintetiese apparaat van die proefplante is bepaal deur analise van chlorofil *a*-fluoressensiekinetika en CO_2-afhanklikheidskrommes (*A*:C_i). Fisiologiese effekte is by *S156* waargeneem lank voor die verkyning van nekrotiese vlekke op die drieledige blare. Fotosintese is aansienlik gerem in *S156*, hoofsaaklik weens ontkoppeling van die suurstofvrystellingskompleks (OEC), remming van fotosintetiese elektronoordrag, gevolglike afname in die reduksie van eind-elektronontvangers (ferredoksien, NADP$^+$) en die gepaardgaande afname in die karboksilering en die regenerering van ribulose-1,5-bisfosfaat. Saad- en peulopbrengs het nou ooreengestem met die fotosintetiese gedrag van die proefplante. Ofskoon blare van albei genotipes sigbaar aangetas was, was dit *S156* wat ernstige nekrotiese vlekke vertoon het. Hierdie data bied nuwe inligting en komplementeer bestaande kennis oor die prosesse onderliggend aan die fitotoksisiteit van O_3, nodig vir die ontwikkeling van bestande genotipes.

Sleutelwoorde: *Phaseolus vulgaris*, osoon, chlorofil *a*-fluoressensie, OEC, PSII, fotosintetiese elektronoordrag, CO_2-assimilering, stomatale geleiding, saadopbrengs, *open-top*-groeikamers.

Introduction

Atmospheric pollution has risen sharply since 1973 due to a drastic increase in commercial energy consumption (McCormick 1997). Some of these emissions, such as CH_4, NO_x, CO and volatile organic carbons (VOCs) are associated with the production of the secondary air pollutant, ozone (O_3) (Monks et al. 2015). The continuous rise of tropospheric O_3 (IPCC 2007) is considered to be one of the major environmental stress factors, causing more damage to crops and forests than any other air pollutant (Ashmore and Bell 1991). The biological effects of O_3 on plants have been studied for more than 60 years (Manning et al. 1972; Heggestad 1991; Davison and Reiling 1995). Although smaller rates of deposition to non-stomatal surfaces occur, O_3 enters the plant mainly through open stomata during daytime (Fowler et al. 2009). O_3, a powerful oxidant, generates toxic free radicals within the apoplast and cell fluids and is responsible for damage to cell metabolism (Mills et al. 2011). While elevated background levels of O_3 are often insufficient to produce visible injury, lower photosynthesis is often reported (Mckee et al. 1997). They ascribed the reduction in net photosynthesis of plants exposed to O_3 for short terms or chronically, to inter alia impairment of stomatal action, inhibition of electron transport and decreased Rubisco activity and content. Measuring the effect of chronic ozone exposure (38-120 $nmol.mol^{-1}$) on soybean, in an open air experiment, the final verdict of Betzelberger et al. (2012) was that because canopy radiation interception, efficiency of photosynthesis and harvest index were all negatively affected, that the attack by this pollutant is multi-faceted.

Ozone tolerance varies widely between species and genotypes. The families Fabaceae and Solanaceae, which include many crop plants, seem to be particularly sensitive (Heagle 1989). Ozone-sensitive and -tolerant cultivars have been reported for many plant species, including bush bean (*Phaseolus vulgaris* L.) (Guzy and Heath 1993). Using chlorophyll *a* fluorescence and leaf gas exchange to study the response to O_3 of the *Phaseolus vulgaris* cultivars Pinto (sensitive) and Groffy (resistant) in a short-term O_3-exposure experiment (80 $nmol.mol^{-1}$, 4h), Guidi et al. (1997) reported constraints on stomatal conductance and quantum efficiency (F_v/F_M), leading to a decrease in the maximum CO_2 assimilation (A_{max}). However, no clear explanation for the differential response was given. Evaluating physiological and biochemical traits that may confer O_3 tolerance in bean cultivars exposed to acute O_3-stress, Guidi et al. (2010) reported that down-regulation of PSII occurred in the tolerant cultivar resulting in protection against the generation of active oxygen species.

Farage et al. (1991) using single acute (200 $nmol.mol^{-1}$, 4-16h) O_3 exposures of wheat, came to the conclusion that the predominant factor and initial cause of O_3-induced reduction in light saturated CO_2 uptake, was a decrease in apparent carboxylation efficiency and that the capacity for ribulose-1,5-bisphosphate (RuBP) regeneration was less affected. In an effort to identify physiological subsystems that may mediate differences in sensitivity to ozone of three bush bean (*Phaseolus vulgaris* L.) genotypes with known differences in sensitivity to O_3 (*S156*, *R123* and *R331*), Flowers et al. (2007) could not resolve the sequence of loss of ribulose-1,5-bisphosphate carboxylase/oxygenase (Rubisco) content or activity and changes in mesophyll conductance, F_o and F_v/F_M. They were of the opinion that constraints on all of these processes could have been the result of general destruction rather than sequential attack on individual subsystems. Flowers et al. (2007) also reported that unstressed *S156* had a higher photosynthetic rate than *R123*, but had no significant capacity to protect Rubisco from attack at high O_3.

Chlorophyll *a* fluorescence induction measurements are widely used to monitor stress. However the analysis of the fluorescence curves often remained limited to the initial rise phase and the maximum (F_M) and the minimum (F_o) of the fluorescence emission.

In our study, we investigated the effect of O_3 on primary photosynthesis by quantification of the OJIP fluorescence curve by the JIP-test and by plotting and analysing fluorescence curves according to different expressions (Strasser et al. 2004; Strasser et al. 2007). This revealed information on the effect of the applied stress on all partial processes of photosynthesis namely, absorption of light energy, trapping of excitation energy, intersystem electron transport and reduction of end-electron acceptors. In parallel, the stress effect was studied by analysis of CO_2 response curves of photosynthesis (A:C_i curves) of the intact leaves, characterising O_3-induced effects on CO_2 assimilation, carboxylation efficiency, Rubisco regeneration and stomatal limitation. The test plants used were the ozone-sensitive (*S156*) and ozone-resistant (*R123*) *Phaseolus vulgaris* genotypes (bush bean) chronically fumigated in well-controlled OTCs over the full growth period. By parallel measurement of chlorophyll *a* fluorescence and photosynthetic gas exchange we intended to obtain a correlation of complementary information of indirect and direct signals on the photosynthetic response of the test plants. Recording in addition chlorophyll content and seed yield of the test plants, allowed comparison of the response of the plants on biophysical, biochemical and physiological level of photosynthesis as well as on seed yield level. The data are intended to complement the existing knowledge of O_3 effects on photosynthesis of crop plants needed for development of tolerant lines.

Materials and Methods

Experimental site and treatments

The study was conducted at the Potchefstroom campus of the North West University in open-top chambers (OTCs), each consisting of a cylindrical aluminium framework with rain cap, covered with transparent PVC sheeting. Four 5 m^3 chambers, ventilated at 1.5 replacements per minute, were used in this study. Two chambers served as control

and were ventilated with charcoal filtered (CF) air. The two treatment chambers were ventilated with air enriched with O_3 provided by an electrical O_3 generator (UV-20 HO, Olgear, Cape Town). Air was provided to the OTCs by means of a large axial fan with variable speed control. The O_3-generator was fitted inside the fan box, providing a constant O_3 supply (3000 mg/h) generated from pure oxygen fed from gas cylinders. The O_3 concentration in the chamber was controlled by means of an overflow valve, to obtain the desired O_3 concentration of 80 nmol.mol^{-1}, within 10% of the target concentration. The test plants were exposed to this elevated concentration for 9 day-light hours per day for the entire growing season (40 days). The O_3 concentration was measured with an ozone monitor (Model 205, 2B Technologies, Inc., Colorado, USA). See Heyneke et al. (2012) for technical details of the OTC system and for a record of diurnal O_3 levels maintained in the treatment OTCs.

Plant material

Two bush bean (*Phaseolus vulgaris* L.) genotypes namely '*S156*' (O_3-sensitive) and '*R123*' (O_3-resistant), selected from '*Oregon 91*' for O_3 sensitivity (Dr. Richard Reinert, USDA, Raleigh, NC), were obtained from Dr. Kent Burkey from USDA Air Quality Research Unit, Raleigh, NC. Two seeds were planted in 16 dm^3 (30 cm diameter) in four pots per genotype per two treatment chambers and two control chambers respectively. The pots were filled with a mixture of sand, soil and vermiculite (1:2:1). The soil mixture was fertilised with a six month slow release fertilizer, Osmocote (13N:13P:13K). Constant water supply to each pot was mediated by glass fibre wicks (Thoenes Dichtungstechnik GmbH, Germany) placed at different levels in the soil of the pots through which water was taken up by capillary action from water reservoirs positioned underneath each pot. This method ensured good control of the water regime of the test plants in an effort to eliminate possible effects of vapour pressure deficit (VPD) through its influence on stomatal conductance affecting access of ozone to the mesophyll of the leaves.

Chlorophyll content index

Chlorophyll content index (CCI) of youngest fully expanded leaves was measured with a hand-held chlorophyll content meter (CCM-200, Opti-Sciences, Inc., USA). Eight measurements were taken per trifoliate leaf of two plants of each treatment.

Photosynthetic gas exchange

Photosynthetic gas exchange was measured with an infrared gas analysis system (CIRAS-2, PP-Systems, Hertz, U.K.) on four randomly selected plants in each chamber of which two replicate measurements were of the sensitive *S156* line, and two were of the resistant *R123* line. A 2.5 cm^2 section of the third fully expanded leaf was clamped into a broad leaf photosynthetic leaf chamber (PLC) with light and temperature control. The leaf in the cuvette was first acclimated at a CO_2 concentration of 360 µmol.mol^{-1} at a saturating net photosynthetic photon flux (1200 µmol m^{-2} s^{-1}) for five minutes to ensure full activation of Rubisco (Taylor and Terry, 1984). Leaf temperature was kept at 26 °C during measurements. After gas exchange reached a steady state, the intercellular CO_2 concentration (C_i) was manipulated by varying ambient CO_2 concentration (C_a). The linear slope of the response curve was determined by lowering C_a in the cuvette from 360 µmol.mol^{-1} in five steps to 200, 100, 50 and 25 µmol.mol^{-1}. C_a was again stabilised at 360 µmol.mol^{-1} to ensure open stomata and to verify the stability of the photosynthetic apparatus. Lastly, C_a was stepped up from 360 µmol.mol^{-1} in four steps to 500, 700, 1000 and 1500 µmol.mol^{-1}, allowing CO_2 assimilation rate (A) vs. intercellular CO_2 concentration (C_i) response curves (A:C_i curves) to be drawn (Singsaas *et al*., 2001). A three minute measuring period at each successive increment was sufficient to attain stable values. The supply functions [$A = g_{CO2}(C_a - C_i)$] corresponding to the demand functions [$A = CE(C_a - \Gamma)$] were drawn by simply joining the value of $C_i = C_a$ (at 360 ppm) on the abscissa to the point giving A_{360} at this value of C_a (Pammenter, 1989). The degree of stomatal limitation of photosynthesis was calculated by the equation: $l = (A_{360} - A_0)/A_0 \times 100$ (Farquhar and Sharkey 1982).

Abbreviations are as follows: A = net photosynthesis; A_{360} = CO_2 assimilation rate at ambient CO_2 concentration; A_0 = CO_2 assimilation rate in absence of stomatal limitation ($C_i \geq 360$ µmol.mol^{-1}); g_{CO2} = stomatal conductance to CO_2; C_a = ambient CO_2 concentration; C_i = intercellular CO_2 concentration; $CE = \delta A/\delta Ci$ = apparent carboxylation efficiency; Γ = CO_2 compensation concentration; E = transpiration rate; ℓ = % stomatal limitation; PFD = photon flux density.

Interpretation of the parameters was done according to Farquhar and Sharkey (1982). We were aware of the fact that the estimated parameter values may differ for the same data set depending on the fitting methods used (Gu et al. 2010).

Chlorophyll *a* fluorescence induction

Chlorophyll *a* fluorescence induction transients were recorded weekly. Six measurements were taken on two leaves of four different plants in the treatment and control OTCs respectively. Measurements were recorded at night on at least one hour dark adapted leaves with a Plant Efficiency Analyser (Handy-PEA, Hansatech Instruments Ltd., Kingslynn, UK). Each induction transient was induced by red light (peak 650 nm) at 2000 µmol photons m^{-2} s^{-1} (sufficient excitation intensity to ensure complete closure of PSII reaction centres to obtain the true fluorescence intensity of F_M) and recorded for 1 second on a 4 mm diameter area of a dark-adapted, attached leaf sample. The recorded OJIP transients were analysed by the JIP-test according to Strasser *et al.* 2004. OJIP refers to the polyphasic fast fluorescence rise from minimal fluorescence intensity at step O (50 µs), through steps J (~2 ms) and I (~30 ms) to maximal fluorescence at step P (~300 ms). The kinetics of the OJIP fluorescence transient of plants have been found to be very sensitive to environmental conditions (Strasser and Strasser 1995; Krüger et al 1997).

The fast phase fluorescence rise (OJIP) occurring within less than a second after illumination of a dark-adapted plant sample, reflects the concentration of primary reduced quinone electron acceptors of PSII in its reduced state (Q_A^-/$Q_{A,\ total}$) in the thylakoid membranes as effected by the kinetics of several different redox reactions taking place in the photosynthetic ET-chain. The JIP-test represents a translation of the original fluorescence data to biophysical parameters that quantify the stepwise flow of energy through PSII at the reaction centre (RC) as well as at the excited cross-section (CS) level (Strasser and Strasser 1995; Force et al. 2003; Strasser et al. 2004). The average values of these parameters were calculated using the computer program "Biolyzer" (http://www.fluoromatics.com). The parameters which all refer to time zero (start of fluorescence induction) are: (i) the specific energy fluxes (per reaction RC, of PSII) for absorption (ABS/RC), trapping (TR_0/RC), electron transport (ET_0/RC) and dissipation at the level of the antenna chlorophylls (DI_0/RC); (ii) the flux ratios or yields, namely, the maximum quantum yield of primary photochemistry ($\varphi_{Po} = TR_0/ABS = F_v/F_M$), the efficiency with which a trapped exciton, having triggered the reduction of Q_A to Q_A^- can move an electron further than Q_A^- into the electron transport chain ($\psi_{Eo} = ET_o/TR_o$), the quantum yield of electron transport ($\varphi_{Eo} = ET_0/ABS = \varphi_{Po} \bullet \psi_o$) and the quantum yield of dissipation ($\varphi_{Do} = DI_o/ABS = (1 - \varphi_{Po})$; (iii) the phenomological energy fluxes (per excited cross-section, CS) for absorption (ABS/CS), trapping (TRo/CS), electron transport (ET_o/CS) and dissipation (DI/CS); (iv) the fraction of active PSII-reaction centres per total absorption (RC/ABS) and per excited cross-section (RC/CS). The initial stage of photosynthetic activity of a RC complex is regulated by four functional steps namely absorption of light energy (ABS), trapping of excitation energy (TR), conversion of excitation energy to electron transport (ET) and reduction of end electron acceptors beyond PSI (RE). A multi-parametric expression, the so called photosynthetic performance index (PI_{total}), reflecting the contribution of these four partial processes, was introduced by Tsimilli-Michael and Strasser (2008) and Yordanov *et al*. (2008):

$$PI_{total} = \frac{\gamma_{RC}}{1-\gamma_{RC}} \cdot \frac{\varphi_{Po}}{1-\varphi_{Po}} \cdot \frac{\psi_{Eo}}{1-\psi_{Eo}} \cdot \frac{\delta_{Ro}}{1-\delta_{Ro}}$$

where γ_{RC} stands for the fraction of chlorophyll molecules which are active reaction centers of PSII. Therefore, $\gamma_{RC}/(1 - \gamma_{RC}) = RC/Chl_{antenna} = RC/ABS$ in the JIP-test terminology. RC/ABS is the fraction of reaction centre chlorophyll (Chl_{RC}) per total chlorophyll ($Chl_{RC} + Chl_{Antenna}$). This expression can be deconvoluted into two JIP-test parameters and estimated from the original fluorescence signals as $RC/ABS = RC/TR_0 \bullet TR_0/ABS = [(F_{2ms} - F_{50\mu s})/4(F_{300\mu s} - F_{50\mu s})] \bullet F_V/F_M$. The factor 4 is used to express the initial rise of the relative variable fluorescence between steps O and P of the OJIP transient (V_{OP}) per 1 ms. The expression RC/ABS shows the contribution to the PI_{total} due to the RC-density relative to all chlorophylls of PSII. The contribution of the light reactions for primary photochemistry is estimated according to the JIP-test as $\varphi_{Po}/(1 - \varphi_{Po}) = TR_0/DI_0 = k_P/k_N = F_V/F_0$. The contribution of electron transport past Q_A is derived as $\psi_o/(1 - \psi_o) = ET_o/(TR_o - ET_o) = (F_M - F_{2ms})/(F_{2ms} - F_{50\mu s})$. The contribution of the reduction of end electron acceptors (finally $NADP^+$) is derived as $\delta_o/(1 - \delta_o) = RE/ABS = (1\text{-}V_I)/(V_I\text{-}V_J) = (F_M - F_{30\mu s})/(F_M\text{-}F_{2ms})$.

Extended analysis of the fluorescence transients was done by calculation of the difference in relative variable fluorescence to present so-called ΔV curves (expressed as V = f(t)), i.e. subtracting normalised variable fluorescence values of the controls of transients normalised between (1) F_o and F_J ($V_{OJ} = (F_t - F_o)/(F_J - F_o)$ and therefore as a function of time, $\Delta V_{OJ} = (V_{OJ\ treatment} - V_{OJ\ control})$; (2) F_J and F_P ($V_{JP} = (F_t - F_J)/(F_P - F_J)$, $\Delta V_{JP} = (V_{JP\ treatment} - V_{JP\ control})$ respectively, from the fluorescence values of their respective treatments (Figure 2b and 2d). The ΔV plots revealed bands hidden in the J and I steps of the fluorescence kinetics which are much richer in information than the original O-J-I-P transients. From these plots, valuable information was obtained regarding the functionality of the OEC (oxygen evolving system), accumulation of electron carriers such as Q_A^- and reduction of end electron acceptors of the photosynthetic ET chain (Strasser et al. 2004).

To fully interpret the effect of O_3 on the kinetics of the I-P fluorescence transients of the test plants, additional normalisations were done to present the relative amplitude of the I-P phase (Figure 2c and 2e).

See Strasser et al. (2004) for a list of the formulae and a glossary of terms used by the JIP-test for the analysis of the OJIP chlorophyll *a* fluorescence transient.

Crop yield

The pods were harvested as soon as they reached maturity. The pods were separated from the plants and dried for 24h at 60 °C or until constant mass. Yield was determined in terms of total pods per plant, number of seeds per pod, total seed per plant and total gram of seed per plant.

Statistical analysis

Statistical analysis was implemented using the 'Statistica' software package for Windows version 6 (StatSoft, Inc., USA). In data sets with parametric distribution, significant differences between treatments were determined using the Students' t-test. In the strict sense the 8 replicate pots per treatment and per genotype used, are pseudo-replicates. Given the size of the OTCs (5 m^3) used and the excellent control of the daily O_3 concentration which was continuously recorded (Heyneke et al. 2012), we are confident that the use of pseudo-replicate pots per treatment and per genotype was adequate for statistical analysis of the differences reported. Using two treatment OTCs per treatment and per control respectively, ensured that the test plants were all exposed to exactly the same O_3 and clean air regime, respectively, over the full growth period.

Results and Discussion

Plant development and foliar injury

After 35 days of O_3 fumigation a marked decrease in growth was evident in the *S156 Phaseolus vulgaris* genotype (treatment O_3S) when compared to the carbon-filtered test plants (treatment FS) (**Figure 1**). In contrast, little visual damage and inhibition of growth were evident compared to its control (O_3R).

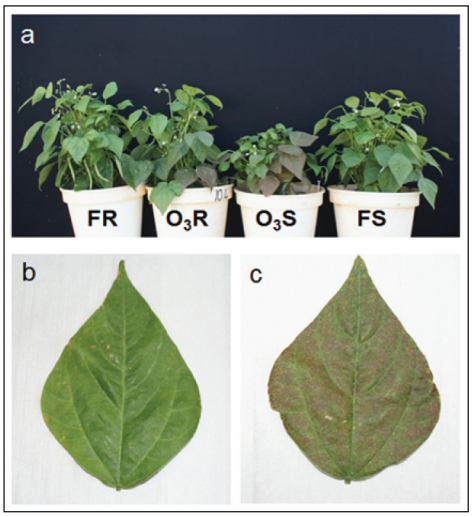

FIGURE 1: (a) Ozone resistant (*R123*) and sensitive (*S156*) *Phaseolus vulgaris* genotypes 35 days after exposure to carbon filtered (F) and 80 nmol.mol^{-1} O_3 respectively. Visual symptoms on leaves after O_3 exposure: **(b)** *R123* plants **(c)** *S156* plants.

Symptoms characteristic of O_3 stress were visible on the *S156* genotype's (O_3S) leaves 12 days after fumigation at 80 O_3 started. Symptoms first appeared as grey/green flecking between the veins, developing into bronze-coloured lesions, which gradually grew together to cover large parts of the leaf surface after 35 days (**Figure 1c**). Burkey et al. (2005) observed similar symptoms in the same genotype. On the other hand the *R123* genotype (O_3R) exposed to the same O_3 concentration, showed far fewer symptoms (**Figure 1b**), which were restricted to older leaves only.

Crop yield

Crop yield attributes were assessed as dry weight at the end of the experiment. Various yield components of the sensitive (*S156*) and resistant (*R123*) genotypes exposed to elevated O_3 concentrations of 80 nmol.mol^{-1} for 40 days, which included the reproductive growth phase, were markedly suppressed when compared to their carbon-filtered controls (**Table I**). The *S156* plants displayed a severe reduction in most of the attributes. The total pods per plant, number of seeds per pod, total seeds per plant and total gram of seed per plant were reduced by 34%, 21%, 51% and 55% respectively. All mentioned differences were statistically significant, with p-values of less than 0.001. The moderate decrease of 21% in seeds per pod in *S156*, indicated that seed initiation was not drastically affected. Although O_3R was less affected in all yield parameters measured, total pods per plant decreased by 16%. The number of seeds per pod, total seeds per plant and total gram of seed per plant, decreased by 21%, 34% and 31%, respectively. It was pointed out that beans (Tingey et al. 2002) and soybean (Morgan et al. 2003) are more vulnerable to O_3 during the reproductive phase than the vegetative phase. The decrease in pod yield in *S156* (O_3S) relative to the control, was comparable to the decrease reported by Burkey et al. (2005) comparing yield of *S156* grown under ambient air containing a seasonal mean of about 50 nmol.mol^{-1} O_3 to those grown under carbon-filtered air. Flowers et al. (2007) exposing *S156* to 60 nmol.mol^{-1} O_3 in OTCs reported a 77% decrease in seed yield.

Physiological response

Chlorophyll *a* fluorescence, difference kinetics and JIP-test

Average chlorophyll *a* fluorescence transients of dark adapted leaves of the test plants are presented on logarithmic time scale in **Figure 2a-c**. These transients show the typical O-J-I-P fluorescence rise, starting from an initial level of F_0, up to a maximum $F_P = F_M$, which can be considered as representing the maximum fluorescence yield, since the intensity of the actinic light source of the fluorimeter (600 W.m^{-2}, peak at 650 nm) is high enough to ensure the closure of all the reaction centres. Important to note is that F_0 and F_M of the chlorophyll *a* fluorescence transients of the test plants were remarkably similar before fumigation commenced, indicating that the plants were physiologically homogenous and active (**Figure 2a**). The similar and low F_0 value furthermore indicated that the plants were fully dark adapted, i.e. all the reaction centres were fully open (oxidised). After 25 days of fumigation with 80 nmol.mol^{-1} O_3, a major treatment effect relative to the control was evident in the OJIP transients of the O_3S plants. **Figure 2b** depicts the average fluorescence transients of the test plants normalised between F_0 (50 µs)

TABLE I: Mean yield parameters (± standard errors) for different treatments measured after seed maturity. Parameters include, total pods per plant, number of seeds per pod, total seed per plant, and total gram of seed per plant, with * and ** indicating significant differences at $p < 0.05$ and $p < 0.01$ respectively, compared to control plants.

Treatments	Total pods	Seeds per pod	Total seeds per plant	Total gram of seed
FR	36.12 (1.43)	3.78 (0.10)	136.87 (7.07)	34.37 (2.13)
O_3R	30.12 (1.12)	2.97 (0.13**)	90.00 (6.04**)	23.42 (1.47**)
FS	38.25 (2.32)	3.25 (0.06)	130.66 (6.60)	31.65 (1.88)
O3S	25.25 (0.97**)	2.55 (0.08**)	64.50 (3.20**)	14.19 (0.93**)

and F_J (2 ms) displaying the events of the O-J and J-P phases of the fluorescence rise respectively. The transition from O to J represents the single turnover range of the transient (i.e. Q_A is only reduced once), reflecting mainly photochemical reactions leading to the reduction of the electron acceptor Q_A, while the transition J to P reflects the multiple turn-over phase which is strongly affected by the subsequent dark reactions in the ET chain. **Figure 2b** suggests that the major O_3-induced effect occurred in the multiple turn-over events of PSII function of the *S156* (O_3S) plants, i.e. in the transition J (~2 ms) to P (~330 ms) (Figure 2b).

Further analysis of the fluorescence transients comprised normalisation of the average fast phase chlorophyll *a* fluorescence transients of the different treatments between the steps O (50 µs) and J (2 ms) as $V_{OJ} = (F_t - F_0)/(F_J - F_0)$, as well as between steps J (2 ms) and F_M (peak), as $V_{JP} = (F_t - F_J)/(F_P - F_J)$. The normalised fluorescence transients of the control (FR) were then subtracted from the normalised fluorescence transients of the different treatments to obtain difference kinetics ($\Delta V = V_{treatment} - V_{control}$), respectively. A gain factor of 6 was used to visualise these differences. The two difference kinetics were then plotted as ΔV_{OJ} and ΔV_{JP}, respectively (ΔV_{OJ} left and ΔV_{JP} right in **Figure 2d**). The positive ΔV_K band (at about 300 µs) appearing in the O_3S plants is the consequence of an increase in fluorescence (**Figure 2d**, left), probably due to the short-lived accumulation of reduced electron carriers such as pheophytin ($Pheo^-$), which, in turn, is caused by the dissociation of the OEC (oxygen evolving complex),

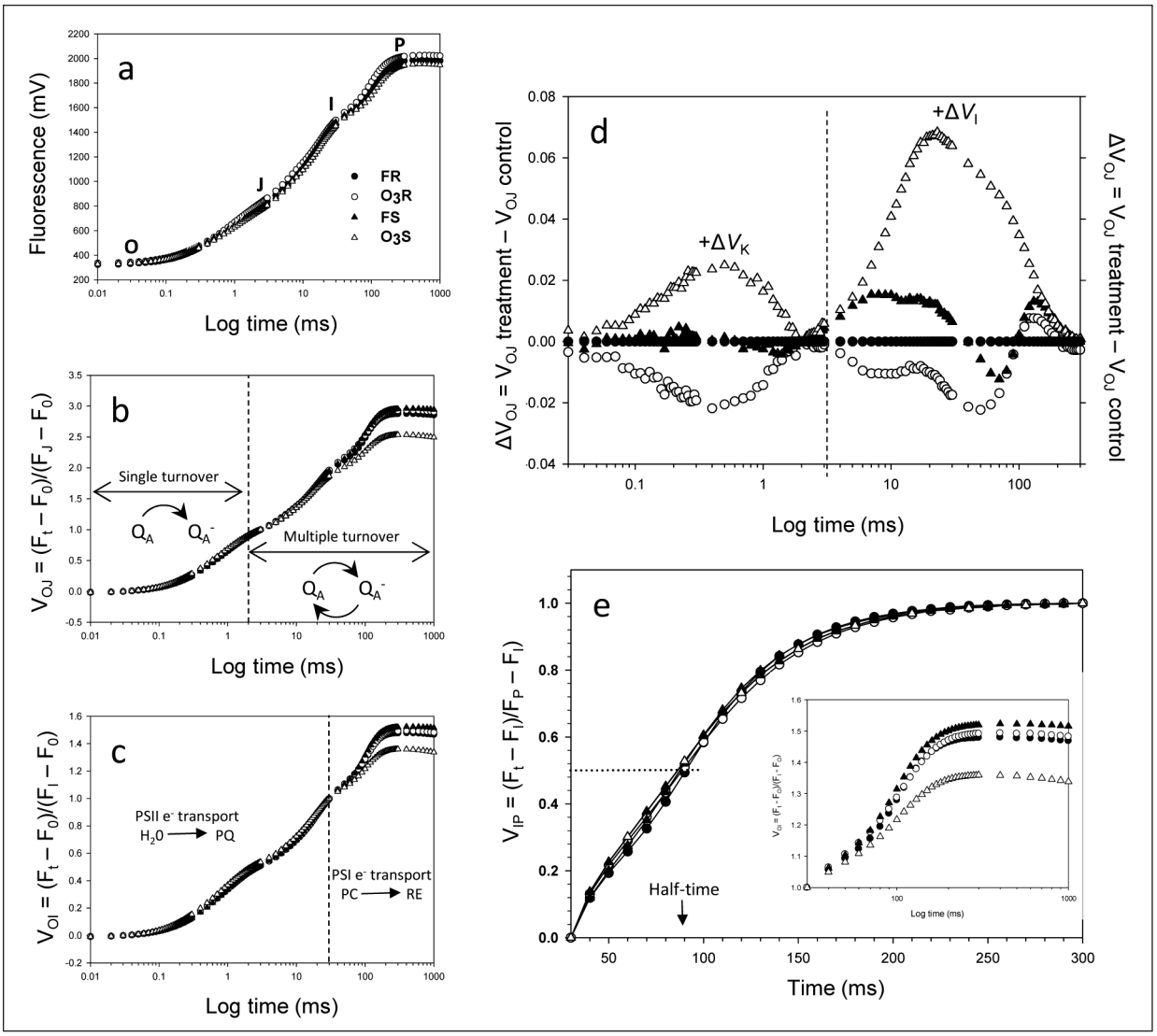

FIGURE 2: Fast phase chlorophyll *a* fluorescence kinetics of intact leaves of the different treatments and genotypes after 25 days exposure to 80 mol.mol^{-1} O_3. **(a):** Averaged unprocessed fluorescence transients before commencement of O_3 exposure; **(b):** Averaged fluorescence transients of intact leaves, double normalised between F_O (50 µs) and F_J (2 ms) on logarithmic time scale, indicating the relative change in the single turnover phase (0 to 2 ms) and the multiple turnover phase (2 ms to ~330 ms); **(c)**: Averaged fluorescence transients of intact leaves double normalised between Fo (50 µs) and F_I (30 ms); **(d)**: Difference in relative variable fluorescence transients ($\Delta V = V_{treatment} - V_{control}$) of different treatments and genotypes (expressed as V = f(t)) normalised between fluorescence extremes F_O (50 µs) and F_J (2 ms) and between F_J (2 ms) and F_P respectively, to obtain the ΔV_{OJ} and ΔV_{JP} curves. ΔV_K and ΔV_I bands are revealed; **(e)**: **insert**: Averaged fluorescence transients normalised between F_O (50 µs) and F_I (30 ms) showing the part V_{OI} for values higher than 1 (after 30 ms) in the time range 30–300 ms (log scale), showing the I-P rise which reflects the size of the end-electron acceptor pool; (e): **main plot**: Averaged fluorescence transients of treatments and genotypes respectively, normalised between F_I (30 ms) and F_M (peak), plotted on a linear scale in the 30–300 ms range with the maximum amplitude fixed at unity (1) for comparing the reduction rate of end-electron acceptors of the different treatments. FR was used as reference/control. Each curve represents the average of 48 measurements.

resulting in an imbalance between the electron flow from the OEC to the RC and towards the acceptor side of PSII. Uncoupling of the OEC enables an alternative internal electron donor such as ascorbate or proline (instead of H_2O) to donate electrons to PSII (Strasser 1974; De Ronde et al. 2004; Toth et al. 2007; Nagy et al. 2012). Such a condition causes a short-lived increase in the reduced Pheo/Q_A^- concentration, creating a ΔV_K-band appearing between 100 and 300 µs. The ΔV_K-band can also occur due to an increase of the functional PSII antenna size (Strasser et al. 2004). On the other hand the O_3R plants displayed a negative ΔV_K-band indicating that in this case the OEC function was not negatively affected relative to the control during vegetative growth, confirming its superb resistance.

A positive ΔV_I-band also became visible between 2 ms and F_M (**Figure 2d**, right) in the O_3S plants after 25 days of exposure to O_3. The ΔV_I-band provides information on the activation state of ferredoxin $NADP^+$ reductase (FNR) and on the possible inhibition of reduction of end electron acceptors such as $NADP^+$ and Fd due to a higher reduced state of the pool mixture of plastoquinone, cytochrome-$_{b/f}$ and plastocyanin (Yusuf et al. 2010). Note that again O_3R was not effected in this regard.

To further elucidate the effect of O_3 on the I-P part of the fluorescence curves, the averaged raw fluorescence curves were normalised between the steps O (50 µs) and I (30 ms) and presented as relative variable fluorescence $V_{OI} = (F_t - F_0)/(F_I - F_0)$ vs logarithmic time (**Figure 2c**). The O-I part of the transient represents the single turnover photochemical event $Q_A \rightarrow Q_A^-$ as well as the beginning of reduction of the intersystem electron carriers, while the I-P part of the transient represents only the PSI-driven reduction of end-electron acceptors, namely Fd and $NADP^+$ (Luo et al. 2006). The marked effect of O_3 on the O-I and I-P phases of the transient of O_3S is depicted by Figure 2c. To reveal the hidden information, two different normalisations of the I-P phase of the transients were used and are presented in **Figure 2e.** The insert represents only the part $V_{OI} \geq 1$ of the normalised curve of **Figure 2c**, plotted in the 30–1000 ms time range (log scale). For each curve, the maximum amplitude of the fluorescence rise reflects the size of the pool of the end electron acceptors at the PSI acceptor side (Yusuf et al. 2010). It is evident that a 10% decrease in the pool size occurred in the O_3S plants, opposed to a 3% increase in the O_3R plants (**Figure 2e, insert**). In the main plot, fluorescence data were normalised between the steps I (30 ms) and P (peak), as $V_{IP} = (F_t - F_I)/(F_P - F_I)$, and plotted on a linear scale in the 30–400 ms range. This normalisation, where the maximal amplitude of the rise was fixed at unity, facilitated a comparison of the reduction rates of the end electron acceptors' pool for the different treatments; their half-times are shown by the interception of the curves with the horizontal dashed line drawn at $V_{IP} = 0.5$ (half-rise). The overall rate constant for reduction of e^--end acceptors can be extrapolated by the inverse of the half-time (Yusuf et al. 2010). No significant changes in the relative reduction rate could be seen in the V_{OP} kinetics of end electron acceptors of the different treatments (**Figure 2e**). Note that Figure 2e (main plot) can be seen as Michaelis-Menten enzyme kinetics V versus S, where the velocity is given by the relative variable fluorescence V_{IP} and the substrate S as the light dose given as the product of light intensity and illumination time.

The comparison of **Figure 2c and 2e** shows that the different phases OJ, JI, and IP of the transient behave differently and carry therefore different information.

The fluorescence transients depicted in **Figure 2b and 2c**, were in addition analysed by the JIP-test (Strasser et al. 2004) to derive 10 structural and functional parameters of PSII function, quantifying the photosynthetic behaviour of the test plants 25 days after fumigation commenced. The values of the parameters are expressed relative to the control (FR) and plotted in a multi-parametric radar plot (**Figure 3**). In the O_3S plants a 13.3% ($p \leq 0.01$) decrease occurred in the number of active reaction centres per absorption (RC/ABS), while a simultaneous 10.8% ($p \leq 0.01$) increase occurred in the apparent antenna size (ABS/RC). The increase in ABS/RC may be due to a compensation strategy to offset the decrease in RC/ABS, resulting in no change in TR_0/ABS (= F_v/F_M) in O_3S (Strasser et al. 2004). The decrease in RC/ABS indicates that the size of the PSII units was affected, but in some of them the reaction centres have been deactivated, hence the corresponding units contributed towards light absorption but not photochemistry (increase of apparent antenna size), or that the size of PSII units with active reaction centres increases (Luo et al. 2006). The 8.07% ($p \leq 0.01$) increase in the maximum trapping flux (TR_0/RC) of the O_3S plants suggests that changes took place both in the fraction of RCs transformed to non-Q_A-reducing RCs and in the functional antenna size (Yusuf et al. 2010). The decrease of 9.53% ($p \leq 0.01$) in the electron transport per cross-section (ET_0/CS) in the O_3S plants can be attributed to a decrease of 9.31% ($p \leq 0.01$) in the density of PSII reaction centres per excited cross section (RC/CS_0). This finding corresponds to the report of Guidi et al. (2010) that down-regulation of PSII activity occurred in beans exposed to acute O_3-stress as protective measure against the generation of active oxygen species.

The O_3-induced changes relative to the control (FR) in the specific (per RC) and phenomenological (per CS) energy fluxes of the O_3S plants were reflected by the 53.5% ($p \leq 0.01$) decrease in the PI_{total}, the latter which provides a measure of the potential of the whole photosynthetic ET chain converting light energy into redox energy (Figure 3). The decreases in the potential of the four partial processes of photosynthesis relative to the control, were as follows: absorption [$\gamma_{RC}/(1-\gamma_{RC}) = RC/ABS$]: 13.7%, trapping [$\varphi_{Po}/(1-\varphi_{Po})$]: 14.5%, electron transport [$\psi_o/(1-\psi_o)$]: 20.8%, reduction of end electron acceptors [$\delta_{Ro}/(1-\delta_{Ro})$]: 22.9%. The large decrease in the potential of the reduction of end-electron acceptors in O_3S (Figure 3), strongly corroborated the data obtained of the difference kinetics of variable fluorescence

transients displaying the prominent ΔV_I-band (Figure 2d). In contrast to the 53.5% decrease in PI_{total} in O_3S, O_3R showed an increase of 18.4% ($p \geq 0.01$), which was mainly due to the higher density of RC/CS and the increased number of active RC/ABS, indicating a stimulatory effect (Figure 3). It should be noted that the parameter $\varphi_{Po} = F_v/F_M$, which is the only fluorescence parameter used in some studies on plant stress effects, was the most insensitive of all parameters. F_v/F_M also proven to be insensitive to drought stress in cotton (Luo et al. 2016).

The changes in structure and function of the photosynthetic apparatus caused by O_3 in the *S123* (O_3S) plants confirmed that considerable injury occurred at the membrane level, specifically regarding the photosystems and redox components of the thylakoids. This could be ascribed to inadequate antioxidant capacity in O_3S in contrast to O_3R, which proved to be well protected

Photosynthetic gas exchange

It is accepted that the most reasonable standard for comparing and characterising the status of the photosynthetic apparatus on the basis of gas exchange is a CO_2 response curve of the intact leaf (Lange et al. 1987). All the measurements shown were done on comparable physiologically active leaves of the different genotypes and treatments after 25 days of exposure. To determine the effect of O_3 on the photosynthetic gas exchange, several photosynthetic gas exchange parameters were derived from the A:C_i response curves (**Figure 4**) and are shown in **Table II**. The actual assimilation rate (ambient conditions, A_{360}), occurs where we find the simultaneous solution of the demand function and the supply function, i.e. the operational point (Figure 4). The A_{360} value of the O_3S test plants decreased by 63 % ($p < 0.01$), while the corresponding small decrease of 3% ($p \geq 0.01$) measured in A_{360} of the O_3R plants showed that O_3 had almost no effect on A_{360} in the *R123* genotype at ambient CO_2 level, corroborating the fluorescence data (PI_{total}, Figure 3). Note that A_{360} in FS was 16 % higher compared to FR, although this phenomenon was not supported by the PI_{total} value (Figure 3). This finding is in accordance with the data of Flowers et al. (2007) showing that *S156* has a higher inherent capacity in clean air as either *R123* or *R331*, but was unable to translate the extra capacity into seed yield. The drastic inhibition of A_{360} (CO_2 assimilation capacity) in the O_3S plants could be ascribed to the decrease in the CO_2 saturated rate of photosynthesis (J_{max}), which indicated that O_3 had an inhibitory effect on the regeneration capacity of RuBP. J_{max} of the sensitive O_3S plants in fact decreased by 61 %. This finding concurs with the explanation of Von Caemmerer and Farquhar (1984), that 'RuBP-regeneration capacity' is more sensitive to stress than Rubisco activity as RuBP regeneration involves the whole biochemistry necessary for photosynthetic carbon assimilation except for one enzyme namely Rubisco. On

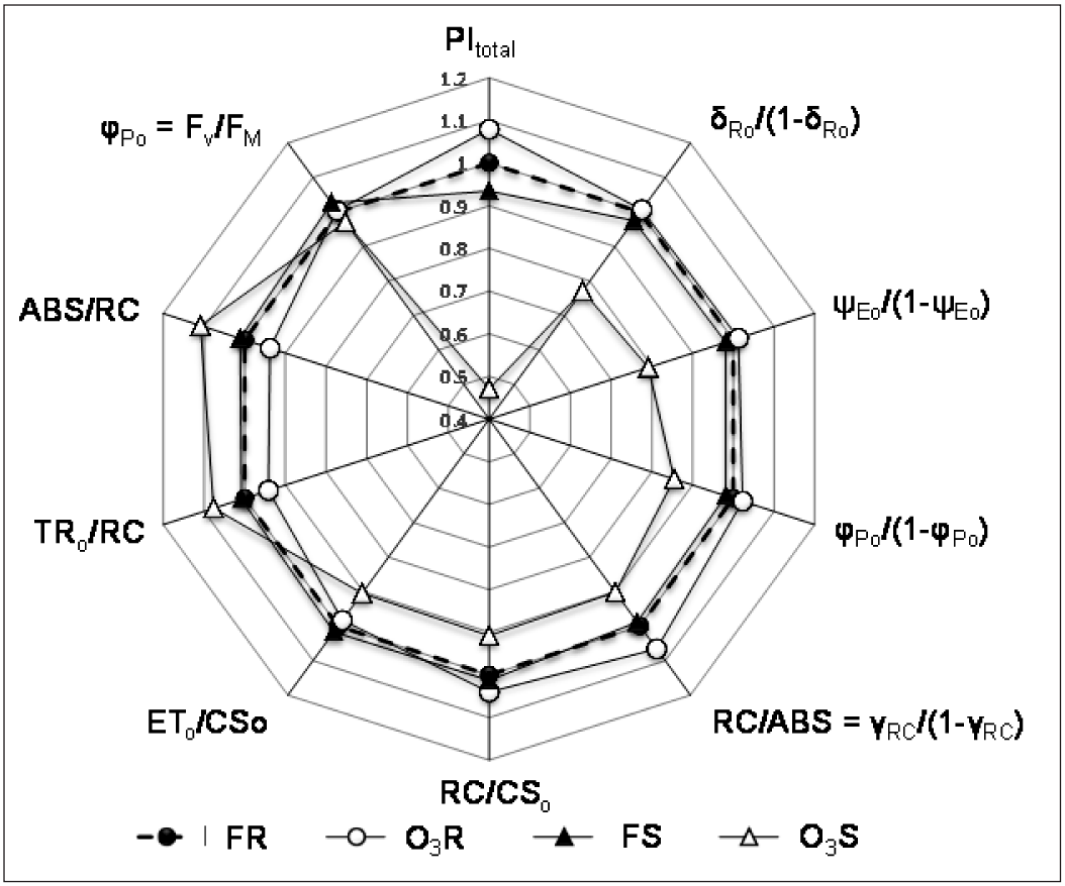

FIGURE 3: Fractional change in selected functional and structural parameters of PSII relative to FR (closed triangles and broken line of regular polygon). O_3R = open circles, FS = closed circles, O_3S = open triangles.

the contrary, J_{max} in O_3R was strikingly unaffected, strongly displaying how well the photosynthetic apparatus of *R123* is protected against O_3 damage.

The carboxylation efficiency (*CE*; initial slope of the *A*:C_i response curve at $C_i \leq 200$ µmol.mol^{-1}) of the O_3S plants decreased by a significant 75 % (Table II). The *CE* expresses the rate of CO_2 assimilation in terms of the effective C_i and the capacity of the system to assimilate CO_2. Farquhar et al (1980) showed that at low *CE*, CO_2 assimilation follows the Michaelis-Menten kinetics and is determined by the RuBP saturated rate of the enzyme: the lower the carboxylation capacity, the less steep the slope of the demand function. The FR and O_3R test plants displayed exactly the same *CE* value (**Figure 4** and **Table 2**), indicating that O_3 had no inhibitory effect on the carboxylation efficiency of the resistant plants exposed to elevated 80 nmol.mol^{-1}, confirming the remarkable O_3-resistance of *R123* genotype reported in literature. Altough *CE* in FS was even slightly higher than in FR, a large decrease occurred in the O_3S plants, corresponding to the contention of Farage et al. (1991), exposing wheat to acute single O_3-doses, that the decrease in *A* was due to decreased *CE*. In contrast to our finding, they however found that J_{max} was less affected. Our data regarding the large difference in sensitivity to O_3 of *R123* and *S156*, corresponded to the findings of Flowers et al. (2007) who came to the conclusion that *R123* compensates for O_3 damage by up-regulating Rubisco activity through either increasing its activation state and/or de novo synthesis. Our gas exchange data fully corroborated the findings of Izuta et al. (1996) working with beech seedlings, that elevated ambient O_3 inhibits both *CE* and J_{max}. An ozone-induced decline in Rubisco activity in sensitive plants was also reported by Pell et al. (1997).

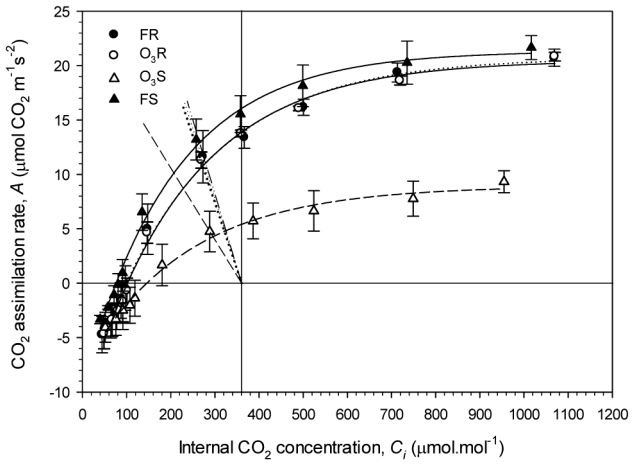

FIGURE 4: CO_2 assimilation rate (*A*) as a function of intercellular CO_2 concentration for leaves of R123 and S156 after 25 days exposure to filtered air (F) and 80 nmol.mol^{-1} ozone (O_3) respectively. Each value represents the mean (± SE) where n = 4. The supply function [$A = g_{CO2}(C_a - C_i)$] corresponding to the demand function [$A = CE(C_a - \Gamma)$] was drawn by simply joining the value of $C_i = C_a = 360$ µmol.mol^{-1} on the abscissa to the point giving A_{360} at this value of C_a (Pammenter 1989). Error bars denote standard error.

The 14% increase in $C_{i\,360}$ of the O_3S test plants, opposed to the 9 % decrease in O_3R, served as further confirmation that the large decrease in A_{360} in O_3S was due to mesophyll limitation rather than stomatal limitation. This fact is corroborated by the 90% increase in Γ (representing the CO_2 compensation concentration) and large decrease (77%) in *CE* in O_3S plants compared to no decrease in O_3R. The supply function (g_{CO2}) in O_3S decreased by 38% ($p < 0.05$). The supply function expresses the rate of CO_2 assimilation in terms of the difference in concentration between C_a and C_i (the driving force for inward movement of CO_2) and the prevailing stomatal conductance (g_{CO2}), however, according to Farquhar and Sharkey (1982) reduced stomatal conductance is rarely the main cause of reduced assimilation rates. Accordingly the moderate 21% increase in *l* calculated for O_3S, confirmed that although stomatal limitation played a role, the reduction in *A* was mainly due to mesophyll limitation. The O_3R plants in contrast displayed a small increase of 9% in *l*. A corresponding decrease of 51% occurred in the water use efficiency (WUE) of O_3S compared to the moderate 7% decrease in O_3R. This decrease in *WUE* occurred in spite of a reduction in transpiration rate (*E*). VanLoocke et al. (2012), exposing soybean to different O_3 concentrations in the range 40 to 120 nmol.mol^{-1} in the Soybean Free Air Concentration Enrichment (SoyFACE)

TABLE 2: Mean values (± standard errors) of photosynthetic gas exchange parameters of leaves of R123 and S156 genotypes (n = 4 plants per treatment) 25 days after commencement of exposure to filtered air (F) and 80 nmol.mol^{-1} ozone (O_3) respectively. Symbols: A_{360} = rate of CO_2 assimilation at $C_a = 360$ µmol.mol^{-1}; $C_{i\,360}$ = intercellular CO_2 concentration at $C_a = 360$ µmol.mol^{-1}; A_0 = rate of CO_2 assimilation at $C_i = 360$ µmol.mol^{-1}; $g_{co2\ 360}$ = stomatal conductance at $C_a = 360$ µmol.mol^{-1}; *CE* = carboxylation efficiency; J_{max} = minimum rate of CO_2 assimilation; Γ = CO_2 compensation concentration; ℓ = percentage stomatal limitation of photosynthesis; *WUE* = water use efficiency. Asterisks * and ** indicate significant differences at $p < 0.05$ and $p < 0.01$, respectively, compared to the control plants (FR).

	FR	O_3R	FS	O_3R
E (mmol.m^{-2}.s^{-1})	5.3 (1.12)	4.66 (0.48)	4.90 (0.86)	3.70 (0.63)
A_{360} (µmol.m^{-2}.s^{-1})	11.45 (1.2)	11.2 (1.2)	13.76 (1.38)	4.92 (1.27**)
$C_{i,\ 360}$ (µmol.mol^{-1})	295.75 (19.34)	270.0 (18.24)	256.16 (18.48)	292.2 (26.61)
A_0 (µmol.m^{-2}.s^{-1})	14.87 (1.24)	14.98 (0.76)	16.07 (0.94)	5.97 (0.85**)
g_{co2} (µmol.m^{-2}.s^{-1})	259 (80.97)	203.25 (25.96)	274.66 (14.71)	165.2 (50.45*)
CE (mol.m^{-2}.s^{-1})	0.056 (0.002)	0.056 (0.002)	0.061 (0.003)	0.014 (0.003**)
J_{max} (µmol.m^{-2}.s^{-1})	20.25 (0.56)	20.17 (0.31)	20.95 (1.27)	7.87 (1.51**)
Γ (µmol.mol^{-1})	98 (4.57)	101.6 (5.64)	76.4 (2.78)	145.8 (6.35**)
ℓ (%)	22.99	25.23	14.37	17.73
WUE (µmol. mmol. $^{-1}$)	2.97 (0.23)	2.75 (0.24)	2.99 (0.13)	1,46 (0.55*)

facility, reported that evapotranspiration decreased linearly with [O_3] and that *WUE* decreased by about 50% which was attributed to O_3-induced limitation of the ability to take up water. Similarly Clebsch et al. (2009) reported a significant reduction in WUE of *Phaseolus vulgaris* Pinto exposed to O_3 in OTCs at concentrations comparable to those used in our study. They attributed the decrease to a larger decrease in *A* relative to a moderate decrease in *E*.

Chlorophyll content index (CCI)

After 30 days of exposure to 80 nmol.mol^{-1} O_3 the O_3S plants showed a 21.8% decrease in the CCI when compared to the FS plants and a 24% decrease compared to FR (**Figure 5**), reflecting the 10% decrease that occurred in the density of RCs (Figure 3). On the contrary the O_3R plants showed a 19% increase in the CCI supporting the 18.4% increase in PI_{total} relative to FR measured in these plants after 25 days exposure (Figure 3). A correlation existed between PI_{total}, and the CCI, both indexes displaying an O_3-induced decrease in O_3S and a moderate increase in O_3R relative to the control. The positive correlation between chlorophyll content and quantum efficiency of photsynthesis is a phenomenon often reported (Nyachiro et al. 2001). The 19% increase found in CCI in O_3R plants, corresponded to the O_3-induced increase found in the clorophyll content of winter wheat in an OTC experiment by Zheng et al. (2005). According to Guzy and Heath (1993) ozone tolerant bean varieties appear to resist chlorophyll loss through mitigation by antioxidants such as ascorbate and non protein sulphydryl. In our investigation the increase in CCI of the O_3R plants was however not reflected in the seed yield. It however must be borne in mind that the values of the yield parameters are the result of the full 40 days of O_3 exposure.

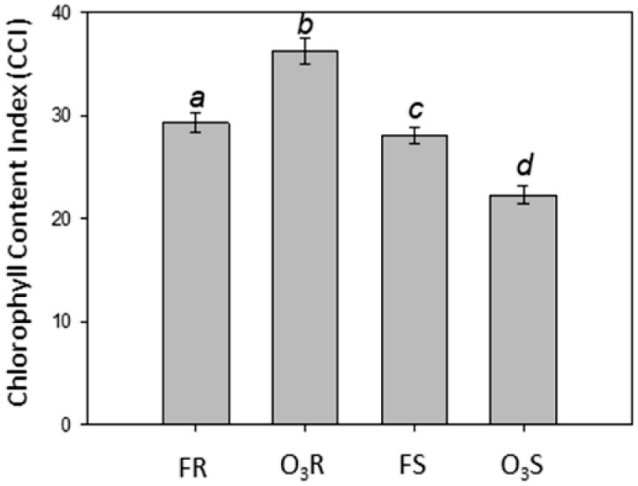

FIGURE 5: Chlorophyll content index (CCI) of R123 and S156 *Phaseolus vulgaris* genotypes after 30 days exposure to carbon filtered air (F) and 80 nmol.mol^{-1} ozone (O_3) respectively. Letters above the error bars indicate the significant differences tested at p = 0.05.

Summary and Conclusions

Exposing the test plants to 80 nmol.mol^{-1} ozone for the full growth cycle up to seed yield showed that the stress imposed was within the physiological capacity of the test plants. This was also supported by the minimal visual effect after 25 days and moderate decrease in yield after 40 days of exposure, respectively, displayed by the resistant (*R123*) genotype.

Our approach of parallel measurement of chlorophyll *a* fluorescence and photosynthetic gas exchange allowed correlation of complementary information of indirect and direct signals on the photosynthetic response of the test plants. Our data convincingly demonstrated that the photochemical processes of the *S156* test plants were not stable against O_3. It is known that O_3-induced altered plasma membrane protein function can serve as initial signals of O_3-responses (Castillo and Heath 1990). It is assumed that thylakoid membranes containing the multi-molecular peptide complexes comprising the photosynthetic electron-transport chain of susceptible plants would be equally subjected to early O_3 damage. Our data suggests that *R123* may be protected by features of their antioxidant metabolism that scavenge O_3-derived ROS (Fiscus et al. 2005). Through analysis of direct chlorophyll fluorescence transients by the JIP test, we could strongly demonstrate that all four domains of the photosynthetic electron transport, namely light absorption (ABS) the PSII electron donor side, electron transport between PSII and PSI, and the PSI electron acceptor side, generating redox energy (reducing equivalents) driving the Calvin-Benson cycle and secondary metabolism, was detrimentally affected in *S156*. By utilisation of the whole fluorescence transient, data were processed indicating that in *S156*, O_3 exposure caused dissociation of the OEC resulting in an imbalance between the electrons flowing from the OEC to the RC and towards the acceptor side of PSII (positive ΔV_K-band). In addition a strong, positive ΔV_I band appeared in the difference fluorescence kinetics, pointing at a decreased activation state of NADP$^+$ reductase and the possible decrease in the reduction of end-electron acceptors (Fd and NADP$^+$). In depth analysis of the I-P phases of the fluorescence transients revealed that in S156 a ~10 % decrease relative to the control (and relative to R*123*) occurred in the pool size of end-electron acceptors. The inhibitory effect of O_3 on photosynthetic electron transport of *S156* was also accompanied by a 24% decrease in the chlorophyll content index (CCI) measured after 30 days of exposure. *R123* proved its resistance to O_3 by not displaying the mentioned effects.

Given the profound inhibitory effects on the functioning of the photosynthetic ET chain in *S156* shown by our data and taking into account that the Calvin-Benson cycle is driven by the reducing equivalents generated by these reactions, we concluded that both the light and dark processes and the interplay between them are attacked by O_3. The large (63 %)

decrease of J_{max} in *S156*, corresponding to the maximum rate of RuBP regeneration and assumed to equal the maximum rate of coupled photosynthetic electron transport (Long and Hällgren 1987), strongly pointed at O_3-induced disruption of the interaction between the Calvin-Benson cycle in the stroma and the ET chain in the thylakoids. What's more, the sensitivity of RuBP-regeneration to O_3 in *S156* is an indication that several enzymes of the Calvin-Benson cycle are affected. The large decrease in *CE* showed that Rubisco was inhibited, either by de-activation, decreased synthesis or degradation.

Although the PI_{total} is an index of photosynthetic potential based on light absorption and measured in the dark-adapted state, it was found to correlate very well with physiological parameters during the vegetative growth stage. Our study demonstrated an excellent correlation between PI_{total} and CO_2 assimilation parameters (*A*, J_{max}, *CE*) measured in the treated plants the following day. Analysing direct fluorescence transients by the JIP test provided a wealth of information on the functionality of the OEC (oxygen evolving system), accumulation of electron carriers such as Q_A^- and reduction of end electron acceptors of the photosynthetic electron transport chain.

Our data confirm the remarkable O_3-resisistance of *R123* during the vegetative growth stage. The extreme sensitivity displayed by *S156* supports its suitability as bio-indicator species as alternative to the clover system as was suggested by Burkey et al. 2005.

Acknowledgements

The authors gratefully acknowledge the North-West University, South Africa, for the funding made available to build the OTC facility. Our research was supported by Sasol Technology (Pty) Limited, and the National Research Foundation (Grant No 77249). The latter included a M.Sc. bursary to CCWS. Dr. Felicity Hayes, Centre for Ecology and Hydrology Wales, Bangor, UK, took the trouble to deliver the valuable seeds used in the experiments to us.

Authors' contribution

CCWS conducted the experiments and wrote a concept article. GHJK designed the experiments and protocol and wrote the final article. RJS contributed to the presentation and interpretation of the chlorophyll *a* fluorescence data. JMB contributed to the finalising of the figures.

References

Ashmore, M.R. and Bell, J.N.B. 1991. The role of ozone in global change. *Annals of Botany,* 67, 39-48.

Betzelberger, A.M., Yendrek, C.R., Sun, J., Leisner, C.P., Nelson, R.L., Ort, D.R., Ainsworth, E.A. 2012. Ozone exposure for U.S. soybean cultivars: Linear reductions in photosynthetic potential, biomass, and yield. *Plant physiology,* 160, 1827-1839.

Burkey, K.O., Miller, J.E., Ficus, E.L. 2005. Assessment of ambient ozone effects on vegetation using snap bean as bioindicator species. *Journal of Environmental Quality*, 34, 1081-1086.

Castillo, F.J. and Heath, R.L. 1990 Ca^{2+} transport in membrane vesicles from pinto bean leaves and its alteration after ozone exposure. *Plant Physiology,* 94, 788-795.

Clebsch, C.C., Divan, A.M., Oliviera, P.L., Nicolau, M. 2009. Physiological disturbances promoted by ozone in five cultivars of Phaseolus vulgaris. *Brazilian Journal of Plant Physiology,* 21, 319-329.

Davison, A.W. and Reiling, K. 1995 A rapid change in ozone resistance of *Plantago major* after summers with high ozone concentrations. *New Phytologist,* 131, 337-344.

De Ronde, J.A., Cress, W.A., Krüger, G.H.J., Strasser, R.J. Van Staden, J. 2004. Photosynthetic response of transgenic soybean plants, containing and Arabidopsis P5CR gene, during heat and drought stress. *Journal of Plant Physiology,* 161, 1211-1224.

Farage, P., Long, S.P., Lechner, E.G., Baker, N. 1991 The sequence of change within the photosynthetic apparatus of wheat following short-term exposure to ozone. *Plant Physiology,* 95, 529-535.

Farquhar, G.D., Von Caemmerer, S., Berry, J.A. 1980. A biochemical model of photosynthetic CO_2 assimilation in leaves of C_3 species. *Planta,* 149, 78-90.

Farquhar, G.D. and Sharkey, T.D. 1982. Stomatal conductance and photosynthesis. *Annual Review of Plant Physiology,* 33, 317-345.

Fiscus, E.L., Booker, F.L., Burkey, K.O. 2005. Crop responses to ozone: uptake, modes of action, carbon assimilation and partitioning. *Plant, Cell and Environment,* 28, 997-1011.

Fowler, D., Pilegaard, K., Sutton, M.A., et al. 2009. Atmospheric composition change. *Atmospheric Environment,* 43, 5193-5267.

Flowers, D., Fiscus, E.L., Burkey, K.O., Booker, F.L., Dubois J-J. B. 2007. Photosynthesis, chlorophyll fluorescence and yield of snap bean (*Phaseolus vulgaris*) genotypes differing in sensitivity to ozone. *Environmental and Experimental Botany,* 61, 190-198.

Force, L., Critchley, C., van Rensen, J.J.S. 2003. New fluorescence parameters for monitoring photosynthesis in plants. *Photosynthesis Research,* 78, 111.

Gu, L., Pallardy, S.G., Tu, K.,Law, B.E., Wullschlegger, S.D. 2010. Reliable estimation of biochemical parameters from C3 leaf photosynthesis-intercellular carbon dioxide response curves. *Plant Cell & Environment,* 33, 1852-1874

Guidi, L., Nali, C., Ciompi, S., Lorenzini, G., Soldatini, G.F. 1997. The use of chlorophyll fluorescence and leaf gas exchange as methods for studying the different responses to ozone of two bean cultivars. *Journal of Experimental Botany*, 48 (306), 173-179.

Guidi, L., Degl'Inocenti, E., Giordano, C., Biricolti, S., Tattini, M. 2010. Ozone tolerance in *Phaseolus vulgaris* depends on more than one mechanism. *Environmental Pollution,* 158, 3164-3171.

Guzy, M.R. and Heath, R.L. 1993. Responses to ozone of varieties of common bean (*Phaseolus vulgaris L.*). *New Phytologist,* 124, 617-625.

Heagle, A.S. 1989. Ozone and crop yield. *Annu Rev Phytopathol,* 27, 397-423.

Heggestad, H.E. 1991. Origen of Bel-W3, Bel-C and Bel-B tobacco varieties and their use as indicators of ozone. *Environmental Pollution,* 74, 264-291.

Heyneke, E., Smit, P.R. Van Rensburg, L., Krüger G.H.J. 2012. Open-top chambers to study air pollution impacts in South Africa. Part I: microclimate in open-top chambers. *South African Journal of Plant and Soil*, 29, 1-7.

IPCC, 2007, Climate change 2007. Impacts, Adaptation, Vulnerability. Contribution of Working Group II to the fourth Assessment Report of the Intergovernmental Panel on Climate Change, Parry, M., Canziani, O., Palutikof, J., Van der Linden, P., Hanson, C. (Eds.), Cambridge University Press, Cambridge, 939 pp.

Izuta, T., Umemoto, M., Horie, K., Aoki, M., Totsuka, T. 1996. Effects of ambient levels of ozone on growth, gas exchange rates and chlorophyll contents *of Fagus crenata* seedlings. *Journal of Japan Society of Atmospheric Environment,* 31, 91-105.

Krüger, G.H.J., Tsimilli Michael, M., Strasser, R.J. 1997. Light stress provokes plastic and elastic modifications in the structure and function of photosystem II in Camelia leaves. *Physiologia Plantarum* 101, 265-277.

Lange, O.L., Harley, P.C., Beyschlag, W., Tenhunen, J.D. 1987. Gas exchange methods for characterizing the impact of stress on leaves. *In* Plant response to stress. *Edited by* J.D.Tenhunen,Springer-Verlag, Heidelberg, Germany, pp 3-22.

Long, S.P. and Hällgren, J-E. 1987. Measurement of CO_2 assimilation by plants in the field and laboratory. *In* J. Coombs, D.O. Hall, S.P. Long, J. M.O. Scurlock (Edit.). Techniques in bioproductivity and photosynthesis. Pergamon Press, pp 62-94.

Luo, H-H., Tsimilli-Michael, M., Zhang, Y-L., Zhang W-F. 2016. Combining gas exchange and chlorophyll a fluorescence measurements to analyze the photosynthetic activity of drip-irrigated cotton under different soil water deficits. *Journal of Integrative Agriculture,* 15(6), 1256–1266.

Luo, T., Deng, W-Y., Chen, F. 2006. Study on cold-resistance ability of Jatropha curcas growing in different ecological environments. *Acta Sci. Nat. Univ. Neimongol,* 37, 446-449.

Manning, W.J., Feder, W.A., Perkins, I. 1972. Sensitivity of spinach cultivars to ozone. *Plant Disease Report,* 56, 832-833.

McCormick, J. 1997. Acid Earth – The politics of acid pollution. 3rd ed., Earthscan Publications Ltd., London, 190 pp.

McKee, I.M., Bullimore, J.F., Long, S.P. 1997. Will elevated CO_2 concentration protect the yield of wheat from ozone damage? *Plant Cell and Environment,* 20, 77-84.

Mills, G., Hayes, F., Simpson, D., Emberson, L., Norris, D., Harmens, H., and Buker, P. 2011. Evidence of widespread effects of ozone on crops and (semi-) natural vegetation in Europe (1990–2006) in relation to AOT40-and flux-based risk maps. *Glob. Change Biol.*, 17, 592–613, doi:10.1111/j.1365-2486.2010.02217.x, 2011

Monks P.S., Archibald, A.T., Colette, A., Cooper, O., Coyle, M., Derwent, R., Fowler, D., Granier, C., Law, K.S., Mills, G.E., Stevenson, D.S., Tarasova, O., Thouret, V., von Schneidemesser, E,. Sommariva, R., Wild, O., Williams, M.L. 2015. Tropospheric ozone and its precursors from the urban to the global scale from air quality to short-lived climate forcer. *Atmospheric Chemistry and Physics*, 15, 8889–8973, 2015, doi:10.5194/acp-15-8889-2015.

Morgan, P.B., Ainsworth, E.A., Long, S.P. 2003. How does elevated ozone impact soybean? A meta-analysis of photosynthesis, growth and yield. *Plant, Cell and Environment,* 26, 1317-1328.

Nagy, V., Tengölics, R., Schansker, G., Rákhely, G., Kovács, K., Garab, G., Tóth, S. Z. 2012. Stimulatory effect of ascorbate, the alternative electron donor of photosystem II, on the hydrogen production of *Chlamydomonas reinhardtii* . *International Journal of Hydrogen Energy,* 37, 8864-8871.

Nyachiro, J.M., Briggs, K.G., Hoddinott, J., Johnson-Flanagen, A.M. 2001 Chlorophyll content, chlorophyll fluorescence and water deficit in spring wheat. *Cereal Research Communications,* 29, No 1/2, 135-142.

Pammenter, N.W. 1989. Clarification of an apparent anomaly in the supply function associated with the response of carbon assimilation to carbon dioxide determined using conventional field equipment. *South African Journal of Science*, 85, 271-272.

Pell, E.J., Schlagnhaufer, C.D., Arteca, R.N. 1997. Ozone-induced oxidative stress: mechanisms of action and reaction. *Plant Physiology,* 100, 264-273.

Singsaas, E., Ort, D.R., Delucia, E.H. 2001 Variation in measured values of photosynthetic quantum yield in ecophysiological studies. *Oecologia*, 128, 15-23.

Strasser, R.J. and Strasser, B. 1995. Measuring fast fluorescence transients to address environmental questions: The JIP-test. In: Mathis, P. (Edit.), Photosynthesis: From Light to Biosphere. Kluwer Academic Publishers, Dortrecht, Vol 5, 977-980.

Strasser R.J. 1974. Studies on the oxygen evolving system in flashed leaves. In: M. Avron, Proceedings of the Third International Congress on Photosynthesis, September 2-6, 1974, Weizmann Institute of Science, Rehovot, Israel. Elsevier Scientific Publishing Company, Amsterdam, The Netherlands.

Strasser, R.J., Srivastava, A., Tsimilli-Michael, M. 2004. Analysis of the chlorophyll *a* fluorescence transient. In: Papageorgiou, G.C., Govindjee (Eds.), Chlorophyll *a* Fluorescence: A Signature of Photosynthesis, pp 321-362.

Strasser, R.J., Tsimilli-Michael, M., Dangre, D., Rai, M. 2007. Biophysical phenomics reveals functional building blocks of plant systems biology: a case study for the evaluation of the impact of mycorrhization with *Piriformaspora indica*. In Varma, A., Oelmüller, R. (Eds.), Soil Biology. Advanced Techniques in Soil Microbiology, volume 11, Springer-Verlag, Berlin.

Taylor, S.E. and Terry, N. 1984. Limiting factors in photosynthesis. V. Photochemical energy supply co-limits photosynthesis at low values intercellular CO_2 concentration. *Plant Physiology,* 75, 82-86.

Tingey, D.T., Rodecap, K.D., Lee, E.H., Hoggset, W.E., Gregg, J.W. 2002. Pod development increases ozone sensitivity of *Phaseolus vulgaris. Water, Air and Soil Pollution,* 39*,* issue 1/4: 325-341

Toth, S.Z., Schansker, G., Garab, G., Strasser, R.J. 2007. Photosynthetic electron transport activity in heat treated barley leaves: The role of internal alternative electron donors to photosystem II. *Biochimica et Biophysica Acta,* 1767, 295-305.

Tsimilli-Michael, M. and Strasser, R.J. 2008. In vivo assessment of stress impact on plant's vitality: applications in detecting and evaluating the beneficial role of mycorrhization on host plants. In: Varma, A. (Ed.), Mycorrhiza: State of the art, Genetics and molecular biology, Eco-function, Biotechnology, Eco-physiology, Structure and systematics, 3rd ed. Springer, pp 679-703.

VanLoocke, A., Betzelberger, A., Ainsworth, E.A., Bernacchi, C.J. 2012. Rising ozone concentrations decrease soybean evapotranspiration and water use efficiency whilst increasingcanopy temperature. *New Phytologist*, 195,

Von Caemmerer, S., Farquhar, G.D. 1984. Effects of partial defoliation, changes of irradiance during growth, short-term water stress and growth at enhanced p(CO_2) on the photosynthetic capacity of leaves of *Phaseolus vulgaris* L.. *Planta* 160, 320-329.

Yordanov, I., Goltsev, V., Stefanov, D., Chernev, P., Zaharieva, I., Kirova, M., Gecheva, V., Strasser, R.J. 2008. Preservation of photosynthetic electron transport from senescence-induced inactivation in primary leaves after decapitation and defoliation of bean plants. *Journal of Plant Physiology,* 165, 1954-1963.

Yusuf, M.A., Kumar, D., Rajwanshi, R., Strasser, R.J., Tsimilli-Michael, M., Govindjee, Sarin, M.B. 2010. Overexpression of γ-tocopherol methyl transferase gene in transgenic *Brassica juncea* plants alleviates abiotic stress: physiological and chlorophyll *a* fluorescence measurements. *Biochimica et Biophysica Acta,* 1797, 1428-1438.

Zheng, Q., Wang, X., Feng, Z., Song, W., Feng, Z. 2005. Ozone effects on chlorophyll content and lipid peroxidation in *in situ* leaves of winter wheat. *Acta Botanica Boreali-Occidentalia Sinica,* 25, 2240-2244.